PROCEDURE TO EVALUATE THE SHEAR RATE PROFILE AND THE APPARENT VISCOSITY OF NON-NEWTONIAN FLUIDS IN THE FALLING CYLINDER VISCOMETER

C.L.A. BERLI[†] and J.A. DEIBER[‡]

†‡ *INTEC (Universidad Nacional del Litoral - CONICET), Güemes 3450, 3000, Santa Fe, Argentina*
† *Dpto. de Física, Fac. de Bioquímica y Cs. Biológicas, UNL, Pje. El Pozo, 3000, Santa Fe, Argentina*
‡ *treoflu@ceride.gov.ar*

Abstract— **The falling cylinder viscometer (FCV) is a reliable instrument to quantify the viscosity of Newtonian fluids. Nevertheless, when non-Newtonian fluids are tested in this device, difficulties appear to determine the apparent viscosity. Thus, conventional rheometric calculations cannot be applied directly to experimental data provided by the FCV in order to obtain the apparent viscosity function, because the knowledge of a rather complex shear rate profile in the annular flow, between the falling cylinder and the container, is required. Consequently, experimental data of the FCV must be processed numerically by including inevitably an appropriate model of the apparent viscosity for the fluid under study. Previous works used the Power Law model, within several small sub-regions of shear rates, selected heuristically, as a reasonable approximation. The present work proposes an algorithm to process the experimental data provided by the FCV for different non-Newtonian fluids. Thus, this generic procedure allows one to perform calculations for any model of the apparent viscosity that includes a set of parameters to be appropriately identified.**

Keywords— **Falling cylinder viscometer, shear rate profile, apparent viscosity, non-Newtonian fluids, ill-posed problem.**

I. INTRODUCTION

Rheometry is based on well known and conventional flow cells, for which theoretical considerations are already set (see, for instance, Walter, 1975; Bird *et al.*, 1977; Tanner, 1985; Macosko, 1994). Falling object viscometers (Fig. 1 illustrates in particular a falling cylinder viscometer) are also proposed in the literature as inexpensive and appropriate instruments to evaluate the apparent viscosity of non-Newtonian fluids. In this sense, the steady state falling velocity U of a given object confined in a tube may be measured and the drag imparted by the surrounding fluid calculated readily, once geometrical scales and density difference $\Delta\rho = \rho_c - \rho$, involving the object density ρ_c and the fluid density ρ, are available. Within this simple experimental framework, the main and difficult problem is to translate the experimental information tabulated as $\{\Delta\rho, U\}$ into the shear-dependent viscosity or apparent viscosity $\eta(\dot{\gamma})$, which is a function of shear rate $\dot{\gamma}$. From previous works, it is clear that apart from the inconvenience that some rheometric cells present non uniform shear rate field (narrow gap concentric cylinders and small angle cone-plate cells are precisely approximations that eliminate this problem), the rheometry associated with falling objects must be complemented with additional theoretical aspects that confront with most rigorous and conventional calculation procedures. One should observe here that conventional rheometric calculations do not apply to the flow kinematics of non-Newtonian fluids generated by falling objects, and the attempt to obtain the apparent viscosity from experimental data involving drag force versus falling velocity requires the knowledge of a shear rate field around any object selected for this purpose. Therefore, the resulting apparent viscosity depends in principle on the constitutive model adopted for an acceptable fitting of experimental results. In this context of calculations, elastic effects may be relevant when the kinematics achieved experimentally is not predominately a shear flow, and hence the rheometric purpose to determine $\eta(\dot{\gamma})$ fails. For instance, the use of a spherical particle falling in a cylindrical tube (falling ball viscometer) is appropriate for Newtonian fluids only. In fact, for the case of non-Newtonian fluids, the mixture of shear and elongational kinematics present around this object introduces an additional complexity associated with elastic effects (see, for example, Zheng *et al.*, 1991).

It is interesting the fact that one can use as falling object a high aspect ratio (slender) cylinder, instead of a sphere, and to present, this is the best alternative for falling object viscometers. Thus, the falling cylinder viscometer (FCV) has become a reliable instrument to quantify the viscosity of Newtonian fluids (Lohrenz *et al.*, 1960; Davis and Brenner, 2001; Cristescu *et al.*, 2002). For this purpose, several studies concerning the computation of end effects (Chen and Swift, 1972; Wehbeh *et al.*, 1993; Park and Irvine, 1995) as well as the introduction of technical improvements for automated measurement (Chan and Jackson, 1985; Ilic and Phan-Thien, 1994; Sha, 1997; Cristescu *et al.*, 2002) have been already published. Concerning non-Newtonian fluids, at present it is known that the FCV appropriately designed may promote a predominant shear flow with negligible elastic effects, because these are confined to

small regions around the cylinder tips. In this regard, the so-called end effects have been always a problem in rheometry and they must be handled with care in all rheometric cells (Walters, 1975). In previous studies Zheng *et al*. (1994) found through a numerical boundary element method that the cylinder aspect ratio (length/radius) must be very high to attain a dominant shear rate kinematics when the material under study is represented through the Phan-Thien and Tanner viscoelastic model. Thus under these conditions the flow problem may be solved approximately as one-dimensional shear flow because near viscometric flow conditions are achieved. Two clear concepts are already available in the literature concerning the use of a FCV for non-Newtonian fluids: (a) the cylinder aspect ratio must be higher than 40, approximately, and (b) a model for the shear-dependent viscosity is required a priori to process experimental data. The last point is conditioned to the first, in the sense that as long as condition (a) is fulfilled, condition (b) within the framework of simple fluid theory of non Newtonian fluids implies simply the knowledge of a model $\eta(\dot{\gamma}, q_1, ..., q_M)$ involving a set of M parameters ($q_1, ..., q_M$) that represents the true apparent viscosity $\eta(\dot{\gamma})$. Relevant to our work here is the fact that this model may not have necessarily a physical meaning; thus $q_1, ..., q_M$ are fitting parameters as the only requirement. Nevertheless, it is also clear that the function $\eta(\dot{\gamma}, q_1, ..., q_M)$ may be obtained conveniently from any inelastic generalized Newtonian fluid (Bird *et al*., 1977) for obvious reasons, independently of the values taken by the first and second normal stress coefficients of the basic viscometric shear flow. This function may be used later as the characteristic apparent viscosity curve coming from the viscometric shear flow test. In this sense, it is also understood that this particular fluid evaluation must be complemented with additional tests like elongational rheometric data, to be able at the end of the characterization process to select the appropriate tensorial viscoelastic constitutive model for the analysis of more complex flows of the fluid under study. Thus, in principle, the tensorial viscoelastic model may be excluded a priori from any analysis of the falling object rheometry if points (a) and (b) described above are effectively achieved, eliminating thus the interpretation of elastic effects associated to data processing from the FCV.

Despite these concepts being well set for an appropriate shear-viscometric flow involving a FCV, the processing of experimental data obtained is a challenging problem at present. In this context, the present work discusses an algorithm to process experimental data from the FCV. Thus, this generic procedure allows one to determine different types of flow curves describing the apparent viscosity that non-Newtonian fluids may usually present. This method also takes advantage of the fact that a function $\eta(\dot{\gamma}, q_1, ..., q_M)$ must be chosen and considered inevitably to perform viscometric calcula-

tions with the FCV. Therefore, by analogy to the treatment of the ill-posed problem in capillary viscometry (Berli and Deiber, 2001; 2004), here we describe a procedure to estimate the parameters ($q_1, ..., q_M$) directly from the experimental data provided as a discrete function $U(\Delta\rho)$. Once the parameter values are calculated, the curve $\eta(\dot{\gamma})$ of the fluid is readily obtained in the range of experimental shear rates achieved with the FCV.

This paper is organized as follows. In Section 2, the equations that govern the shear flow in the FCV are outlined, and the calculations difficulties related to this rheometric cell are described. In Section 3, the procedure suggested in this work is presented first to show how the direct problem involving the calculation of the velocity field in the FCV for a characterized fluid may be performed. Consequently, in Section 4, the shear rate and velocity profiles of different type of fluids in the annular flow of the FCV are presented and discussed. Then, Section 5 considers the inverse problem, which deals with the parameter identification of the apparent viscosity function proposed by using experimental data from the FCV. For this purpose, the procedure is also described in details and relevant examples are included to illustrate the salient advantages of these calculations.
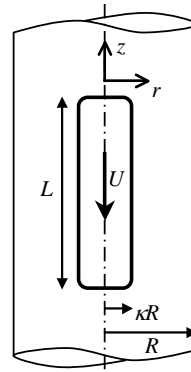

Figure 1. Schematic representation of the FCV including the coordinate system used in calculations.

II. THEORY

A. Basic Equations

For the purposes of the theoretical analysis in this section, the basic geometry of the FCV is shown schematically in Fig. 1, where a cylindrical coordinate system is used. The experimental features of this device are well documented in the literature (Cristescu *et al*., 2002; Chan and Jackson, 1985; Cho *et al*., 1992; Ilic and Phan-Thien, 1994; Sha, 1997). The aspect ratio $L/\kappa R$ must be higher than 40 to provide unidirectional flow throughout the annular space between the cylinder and the confining tube (the effect of the aspect ratio on the flow field has been discussed in the literature; Cho *et al*., 1992; Zheng *et al*., 1994). This requirement assures that end effects are negligible (Park and Irvine, 1995). Under these conditions it is assumed that the axial com-

ponent of fluid velocity $u_z(r)$ varies with the radial coordinate r only. When the falling cylinder reaches the terminal velocity U, the shear stress τ_{rz} in the fluid satisfies the following axial component of momentum balance (Walters, 1975; Bird *et al.*, 1977):

$$\frac{1}{r}\frac{\partial(r\tau_{rz})}{\partial r} = -\frac{\partial(p-\rho g z)}{\partial z} , \qquad (1)$$

where p is the pressure, g is the gravitational acceleration, z is the axial coordinate and the term $-\partial(p-\rho g z)/\partial z = \Delta P/L$ is the generalized pressure drop along the cylinder. Integrating Eq. (1) to find τ_{rz} requires a boundary condition, which is obtained through a force balance carried out on the falling cylinder in steady state, yielding,

$$\Delta\rho\, g = \frac{2\tau_{\kappa R}}{\kappa R} + \frac{\Delta P}{L} , \qquad (2)$$

where $\tau_{\kappa R} = \tau_{rz}(\kappa R)$ is the shear stress at the cylinder wall. Equation (2) is quite general in the sense that, when additional fields are applied in the axial direction, namely magnetic forces, the density difference $\Delta\rho$ must include the term accounting for the "local density" associated with this field (Cristescu *et al.*, 2002). Therefore, Eqs. (1) and (2) with the definition of ΔP yield the following expression for the shear stress at any posistion r,

$$\tau_{rz}(r) = \tau_{\kappa R}\frac{r}{\kappa R} + \frac{\Delta\rho\, g\kappa R}{2}\left(\frac{r}{\kappa R} - \frac{\kappa R}{r}\right). \qquad (3)$$

This equation can be equivalently written in terms of ΔP instead of $\tau_{\kappa R}$. However, it is worth observing that neither $\tau_{\kappa R}$ nor ΔP are accessible experimentally. Also under steady state conditions, and considering non-slip of the fluid at the walls, the boundary conditions for the fluid velocity are,

$$u_z(\kappa R) = -U , \qquad (4)$$

$$u_z(R) = 0 . \qquad (5)$$

In addition, since the bottom of the fluid container is closed, a mass balance in the flow domain provides the following relation between the cylinder velocity U and the fluid velocity $u_z(r)$:

$$U(\kappa R)^2 = 2\int_{\kappa R}^{R} u_z(r)\, r\, dr . \qquad (6)$$

B. The Ill-Posed Equations

Given the equations that govern the unidirectional flow in the annular space of the FCV, and following the framework of conventional rheometry, one should find expressions for τ and $\dot\gamma$ in terms of U and $\Delta\rho$, in order to calculate $\eta(\dot\gamma) = \tau/\dot\gamma$ for the fluid tested. Although the shear stress is explicitly given by Eq. (3), it cannot be quantified at any place in the flow domain because $\tau_{\kappa R}$ (or, equivalently, ΔP) is not known from the experiment. In addition, for the shear flow considered

here, the shear rate is $\dot\gamma = |\dot\gamma_{rz}|$, where $\dot\gamma_{rz} = -\partial u_z/\partial r$ is the fluid velocity gradient. By using this definition, Eqs. (4)-(6) yield (Eichstadt and Swift, 1966; Phan-Thien *et al.*, 1993),

$$\int_{\kappa R}^{R} \dot\gamma_{rz}(r)\, r^2\, dr = 0 , \qquad (7)$$

$$\int_{\kappa R}^{R} \dot\gamma_{rz}(r)\, dr = -U . \qquad (8)$$

Nevertheless, any attempt to calculate the shear rate from Eqs. (7) and (8) requires the knowledge of either $\dot\gamma_{\kappa R} = \dot\gamma_{rz}(\kappa R)$ or $\dot\gamma_R = \dot\gamma_{rz}(R)$. This difficulty is analogous to that appearing in Couette viscometry (Walters, 1975; Bird *et al.*, 1977; Macosko, 1994).

In addition, it should be observed that, as it happens in capillary viscometry, the shear rate attained in the annular flow of the FCV is not uniform throughout the flow domain. Therefore, the equations relating $\dot\gamma$ to the measured variables cannot be solved in a straightforward calculation. Indeed, extracting $\dot\gamma$ from Eq. (8) requires inverting the integral equation, the solution of which is not unique due to the scattering present in the experimental data. For this reason, the problem is also qualified as "ill posed" in the literature (see, for instance, Friedrich *et al.*, 1996; Berli and Deiber, 2001).

C. Relevant Prior Work to Evaluate the Apparent Viscosity in the FCV

In order to overcome the difficulties associated with the FCV, Ashare *et al.* (1965) considered the limiting situation where both the annular gap width and the cylinder velocity were very small. Only in this asymptotic case, τ and $\dot\gamma$ can be directly calculated from U and $\Delta\rho$ as follows:

$$\tau_R = \frac{\Delta\rho\, R\, g}{2}\left(\varepsilon - \varepsilon^2 - \frac{\varepsilon^3}{2} - \frac{\varepsilon^5}{4} + ...\right), \qquad (9)$$

$$\dot\gamma_R = \frac{U}{R\varepsilon^2}\left(2 + \frac{d\ln U}{d\ln\tau_R}\right)\left(1 - \frac{\varepsilon}{2} - \frac{\varepsilon^2}{10} - \frac{\varepsilon^3}{20} + ...\right), \qquad (10)$$

where $\varepsilon = (1-\kappa)$ and the subscript R indicates that these variables are evaluated at the container wall. These equations are strictly valid for experiments carried out with $\varepsilon \to 0$ and $U \to 0$. In addition, the numerical results yielded by Eq. (10) are very sensitive to the way the derivative $d\ln U/d\ln\tau_R$ is numerically calculated, because experimental data are always noisy in some degree.

On the other hand, as explained above, to carry out calculations for general values of ε and U, a relationship between τ and $\dot\gamma$ must be introduced beforehand. In this sense, Eichstadt and Swift (1966) solved the flow field in the annular space for the particular cases of Power Law (PL) and Bingham fluids. This theoretical approach has been reworked later (Park and Irvine, 1988; Cho *et al.*, 1992), where extensive tables of numerical data

concerning the PL fluid were reported to facilitate the estimation of $\eta(\dot{\gamma})$ with the FCV.

Phan-Thien *et al.* (1993), and then Zheng *et al.* (1994), also exploited the PL model to analyze non-Newtonian fluids in this viscometer. Important in this work is that the procedure is also aimed to be applied to different fluids for which the viscosity curve can be divided into several sub-regions, each one with a local PL behavior (this practice has been already used in capillary viscometry in relation to an ill-posed problem similar to that mentioned above). Thus, the equation deduced by these authors that must fit the sub-regions of experimental data $\{\Delta\rho,U\}$ is,

$$\frac{D\,\mu}{D_N} = m\left(K\,\frac{U}{R}\right)^{n-1}, \qquad (11)$$

where $D = \Delta\rho g (\kappa R)^2 \pi L$ is the drag force on the cylinder, D_N is the respective value for a Newtonian fluid of viscosity μ (see Appendix A) and parameters m and n are the fitting parameters (see also Table 1). It is also shown that the left hand side of Eq. (11) is equal to the viscosity function $\eta(\dot{\gamma})$, whereas KU/R is the effective shear rate. To use quantitatively this expression, the constant K is obtained from semi-empirical relations as follows: $\log K = b_0 - b_1 \log n$, $b_0 = 0.45790 + 3.2305(\kappa - 0.1)^2$ and $b_1 = 0.070437\kappa^{-0.585}$ (Phan-Thien *et al.*, 1993; Zheng *et al.*, 1994). These relations apply when $0.1 \le n \le 0.9$ and $0.05 \le \kappa \le 0.3$ with an estimated error less than 1.8% (see also in Section 5.4 the systematic deviation from the expected flow curve that this method introduces). Although this technique appears to be a good approximation, the particular method of data processing provides results for PL pseudoplastic fluids only, and it is limited to a small range of κ.

Therefore, a simpler and accurate procedure to determine directly the viscosity function of non-Newtonian fluids would be in addition desirable for practical reasons. Having as reference point this last conclusion, this work proposes an algorithm to process data $\{\Delta\rho,U\}$ for different non-Newtonian fluids. This algorithm has been designed to employ a generic function of the apparent viscosity. The associated iterative procedure avoids the use of pre-fitted semi empirical equations based on one specific model and is valid for any value of κ.

III. PROCEDURE SUGGESTED

As discussed above, the only possibility to perform viscometric calculations in the FCV is to include additional information about the fluid, namely, a relationship between τ_{rz} and $\dot{\gamma}_{rz}$ in the form,

$$\tau_{rz} = \eta(\dot{\gamma}, q_1, ..., q_M)\dot{\gamma}_{rz}, \qquad (12)$$

typical examples of this function are listed in Table 1, corresponding to the generalized Newtonian fluid for practical reasons. The function $\eta(\dot{\gamma}, q_1, ..., q_M)$ may be also obtained from a tensorial constitutive model evaluated for the shear flow kinematics, i.e., $q_1, ..., q_M$ may be actual rheological parameters, although this interpretation depends on the final tensorial model to be assigned to the fluid and it is not necessarily a requirement. It should be observed that only the apparent viscosity is evaluated here, which is one of several steps in the complex rheological process of fluid characterization. Therefore after combing Eqs. (3) and (12), the following generic expression is derived

$$\eta\left[\dot{\gamma}(r), q_1, ..., q_M\right]\dot{\gamma}_{rz}(r) = \tau_{\kappa R}\frac{r}{\kappa R} + \frac{\Delta\rho\,g\kappa R}{2}\left(\frac{r}{\kappa R} - \frac{\kappa R}{r}\right). \qquad (13)$$

Therefore, the shear flow developed in the FCV is described by the set of coupled Eqs. (7), (8) and (13), which derive from the momentum and mass balances in the fluid, with the apparent viscosity model selected. It is relevant to add here that the flow in the annular gap between the cylinders depends on the apparent viscosity function only, independently of the existence of normal stress differences in the fluid, provided that $L/\kappa R$ is higher than 40, approximately (Zheng *et al.*, 1994). This constraint assures that the flow is near unidirectional along the annular space, and hence both $\dot{\gamma}_{rz}(r)$ and $\tau_{rz}(r)$ vary in the radial direction only. Of course, the other experimental requisites to attain a viscometric flow in the cell must be also satisfied: steady state, isothermal flow, no-slip at the walls, and end effects negligible (Walter, 1975; Bird *et al.*, 1977). Under these conditions, the FCV can be used to evaluate the apparent viscosity of a non-Newtonian fluid, regardless of its possible viscoelastic properties (Zheng *et al.*, 1994).

Table 1. Expressions of the apparent viscosity associated with typical models (Bird et al., 1977).

Function $\eta(\dot{\gamma})$		Parameter designations
I	q_1	Newton:
		$q_1 = \mu$ (viscosity coefficient)
II	$q_1\dot{\gamma}^{q_2-1}$	Power Law:
		$q_1 = m$ (consistency)
		$q_2 = n$ (flow index)
III	$q_1 + \dfrac{q_2}{\dot{\gamma}}, \ \tau > q_2$	Bingham:
		$q_1 = \eta_p$ (plastic viscosity)
		$q_2 = \tau_p$ (yield stress)
IV	$\dfrac{q_1 - q_4}{1 + (q_2\dot{\gamma})^{q_3}} + q_4$	Cross (Cross, 1965):
		$q_1 = \eta_0$ (low-shear viscosity)
		$q_2 = \lambda$ (relaxation time)
		$q_3 = \alpha$ (positive index)
		$q_4 = \eta_\infty$ (high-shear viscosity)

The solution of the algebraic problem defined by Eqs. (7), (8) and (13) requires a numerical algorithm, except in the case of Newtonian fluids (see Appendix A). Further, for a general function $\eta(\dot{\gamma}, q_1, ..., q_M)$, calculations may be performed in two different ways:

a) If the parameter values in $\eta(\dot{\gamma}, q_1, ..., q_M)$ for a particular fluid are available, one may obtain $\dot{\gamma}_{rz}(r)$, U and $\tau_{\kappa R}$ (3 unknowns), for given values of $\Delta\rho$, κ and R (designated direct problem). These calculations basically concern the dynamics of non-Newtonian fluids in the annular space of the FCV, and will be considered below in Section 4 to examine the behavior of typical fluids in this type of rheometric cell.

b) On the other hand, if data U vs. $\Delta\rho$ are obtained in a FCV, Eqs. (7), (8) and (13) allow one to estimate the M unknown parameters pertaining to the function $\eta(\dot{\gamma}, q_1, ..., q_M)$ appropriately chosen for the fluid under study (designated inverse problem). In this case, as the unknowns are $\dot{\gamma}_{rz}(r)$, $\tau_{\kappa R}$ and the M model parameters, at least M pairs of data U vs. $\Delta\rho$ are needed. These calculations are of interest to carry out the viscometric test in the FCV and constitute the main objective of this work (Section 5).

IV. ANALYSIS OF THE SHEAR RATE IN THE ANNULAR FLOW (DIRECT PROBLEM)

A. Calculation Scheme

The aim of this section is to calculate the shear rate profile, as well as to visualize the behavior of typical fluids in the annular flow of the FCV, before presenting the determination of parameters $(q_1, ..., q_M)$. In this sense, a calculation scheme to solve the set of Eqs. (7), (8) and (13) for a given fluid with a known viscosity function is described. Therefore once the viscosity model and related parameters are specified, the first step consists in finding $\dot{\gamma}_{rz}(r)$ as numerical roots of Eq. (13), for defined values of $\Delta\rho$, κ and R. This task is carried out through a Newton-Raphson subroutine (Carnahan et al., 1969), for around 10^4 discrete values of r in the range $\kappa R \le r \le R$. Since the unknown τ_{rz} enters these calculations, an iterative process is conducted by starting with an initial guess obtained from Eq. (A3). A Newton-Raphson subroutine is also used to correct the value of $\tau_{\kappa R}$ at each iteration, until $\dot{\gamma}_{rz}(r)$ satisfies Eq. (7) for a certain relative error of the order of 10^{-5}. When the convergence criterion is reached, the roots $\dot{\gamma}_{rz}(r)$ at discrete values of r are attained and hence U may be calculated from Eq. (8). The velocity $u_z(r)$ is also calculated by integrating $\dot{\gamma}_{rz}(r) = -\partial u_z/\partial r$ from κR to R. A simple crosscheck for these calculations can be carried out as follows: the function $\eta = \tau_{\kappa R}/\dot{\gamma}_{\kappa R}$, with values $\tau_{\kappa R}$ and $\dot{\gamma}_{\kappa R}$ obtained numerically, must match the apparent viscosity $\eta(\dot{\gamma}, q_1, ..., q_M)$, which is an input in the algorithm for this case.

B. Shear Flow Behavior of Typical Fluids

Results obtained with Functions III and IV of Table 1 are presented here, as examples of non-Newtonian behavior. In particular, the PL fluid (Function II) has been well described elsewhere (Park and Irvine, 1988; Cho et al., 1992; Phan-Thien et al., 1993; Zheng et al., 1994). The parameter values used for Function III were $q_1 = 0.1$ Pa s and $q_2 = 0.08$ Pa, while for Function IV were $q_1 = 0.1$ Pa s, $q_2 = 0.05$ s, $q_3 = 1$ and $q_4 = 0$. The mathematical problem described above (Eqs. (7), (8) and (13)) has been solved for these fluids by assigning different values to $\Delta\rho$ in the range 10-4000 kg/m³, and considering a viscometer with $\kappa = 0.25$ and $R = 0.005$ m. Shear rate and velocity profiles are shown in Figs. 2 (a) and (b), respectively, where the Newtonian solution is also included for comparison (Function I, Eq. (A1)). The flow curves corresponding to Function IV show a typical pseudoplastic behavior, with the velocity profile shifted to the falling cylinder wall, where the shear rate is relatively high. For Function III, which predicts plastic behavior, a plug flow is observed in the region where $\tau_{rz}(r)$ is lower than $q_2 = 0.08$ Pa.
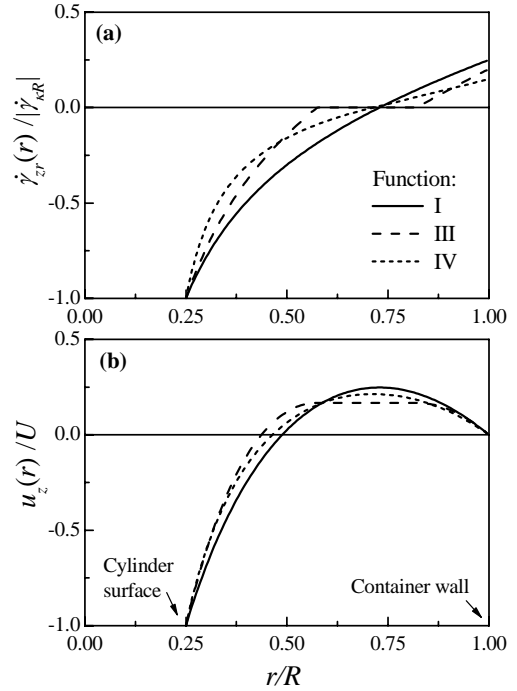

Figure 2. (a) Shear rate and (b) velocity profiles, as a function of the radial coordinate in the annular gap between cylinders. Geometrical characteristics used in calculations are $R = 0.005$ m and $\kappa = 0.25$. In particular, $\Delta\rho = 100$ kg/m³ in the case of Function III and 200 kg/m³ in the case of Function IV. The parameter values of the viscosity functions are reported in the text.
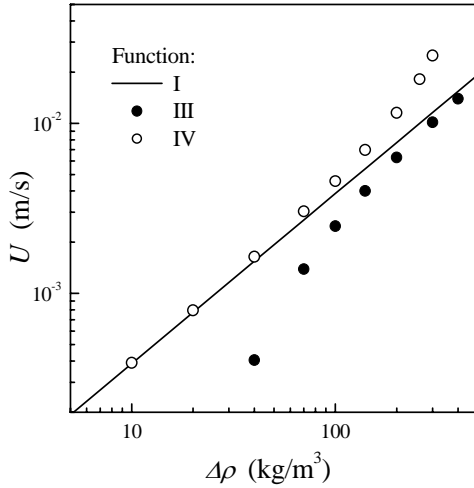
Figure 3. Terminal velocity of the falling cylinder as a function of the density difference, for $R = 0.005$ m and $\kappa = 0.25$. The parameter values are reported in the text. The line representing the Newtonian fluid is obtained from Eq. (A2) with $\mu = 0.1$ Pa s.

Figure 3 presents the resulting falling cylinder velocity U for each value of $\Delta\rho$ used as input in the algorithm. Once more the solution for a Newtonian fluid (Function I) has been included as a reference (straight line, from Eq. (A2) with $\mu = 0.1$ Pa s). This figure shows how the terminal velocities predicted by Functions III and IV deviate from that of the Newtonian fluid (the same value of q_1 has been chosen here for all the fluids under analysis). In particular, for Function III, the velocity U decreases rapidly as $\Delta\rho$ decreases, and eventually vanishes for a critical value of $\Delta\rho$ at which the material virtually becomes a solid. Therefore, the curve $U(\Delta\rho)$ provides a relevant information concerning the rheological response of the fluid tested. In relation to the analysis reported in previous works (Park and Irvine, 1988; Cho *et al*., 1992; Phan-Thien *et al*., 1993; Zheng *et al*., 1994), one finds that the PL fluid always yields straight lines in log-log plots of U vs. $\Delta\rho$, the slopes of which depend on the flow index n and on the selection of the different shear rate zones.

It is relevant to mention here that the geometric scales selected for the numerical examples are typical values used in experiments, and although the length L does not enter explicitly in calculations, the condition $L/\kappa R > 40$ is easily attained in practice. For example, for the above values of κ and R, a cylinder with $L > 0.05$ m yields $L/\kappa R > 40$. These high values of the aspect ratio assure that (a) the elasticity of the fluid does not affect the shear stresses on the cylinder (Zheng *et al*., 1994), and (b) errors due to end effects are minimized (Park and Irvine, 1995). In this sense, the pairs U vs. $\Delta\rho$ reported in Fig. 3 can be regarded as pseudo-experimental data for the fluids considered, since the calculations emulate ideal experiments with the FCV.

V. CALCULATION OF THE VISCOSITY FUNCTION (INVERSE PROBLEM)

A. Procedure

In this section the inverse problem is studied, which consists in determining the unknown parameters of the apparent viscosity (the proposed function) from data U^{ex} vs. $\Delta\rho^{ex}$. The superscript *ex* refers here to experimental data obtained in the FCV with the requirement $L/\kappa R > 40$. As mentioned above, the curve $U^{ex}(\Delta\rho^{ex})$ is used here within the theoretical framework presented by Eqs. (7), (8) and (13), which must include a viscosity model $\eta(\dot{\gamma}, q_1, ..., q_M)$ appropriately selected for the fluid under study. Therefore one can estimate parameters $q_1, ..., q_M$ of the selected model by fitting the theoretical function $U(\Delta\rho, q_1, ..., q_M)$ to the curve $U^{ex}(\Delta\rho^{ex})$. Once the best values estimated of $q_1, ..., q_M$ are obtained, $\eta(\dot{\gamma})$ can be readily calculated in the range of shear rates obtained experimentally with the FCV.

A crucial aspect here is that Eqs. (7), (8) and (13) cannot be abridged into a single expression of the form $U(\Delta\rho, q_1, ..., q_M)$, except in the case of Newtonian fluids only (Eq. (A2)). Therefore, for a given viscosity model, the function $U(\Delta\rho, q_1, ..., q_M)$ must be obtained numerically and then fitted to the curve $U^{ex}(\Delta\rho^{ex})$. To perform these calculations, we developed an algorithm in which the inputs are N pairs $\{U^{ex}, \Delta\rho^{ex}\}$ and the initial guess $q_1^a, ..., q_M^a$, while the output are the best values estimated for $q_1, ..., q_M$ characterizing the apparent viscosity for the fluid under study, as shown in the diagram of Fig. 4.

The calculation procedure is basically the following: for each data $\Delta\rho_i^{ex}$, from $i = 1$ to N, the profiles $\dot{\gamma}_{rz}(r)$ corresponding to the selected function $\eta(\dot{\gamma}, q_1, ..., q_M)$ are obtained. Then $U_i(\Delta\rho_i^{ex})$ is calculated through Eq. (8). To identify the best parameter values, the sum of differences,

$$S = \sum_{i=1}^{N} \left(\frac{U_i(\Delta\rho_i^{ex}, q_1, ..., q_M) - U_i^{ex}}{U_i^{ex}} \right)^2, \qquad (14)$$

is minimized through an iterative process, following the outer loop indicated in Fig. 4. Therefore, the calculation involves a subroutine (Appendix B) designed to solve a system of M non-linear algebraic equations, which comes from the requirement of minimizing S as a function of the M model parameters. As mentioned above, the minimum number of experimental data required to solve this algebraic problem is equal to the number of model parameters. Further, in order to attain a statistically meaningful solution, the degrees of freedom $N-M$ should be higher than M (Carnahan *et al*., 1969).
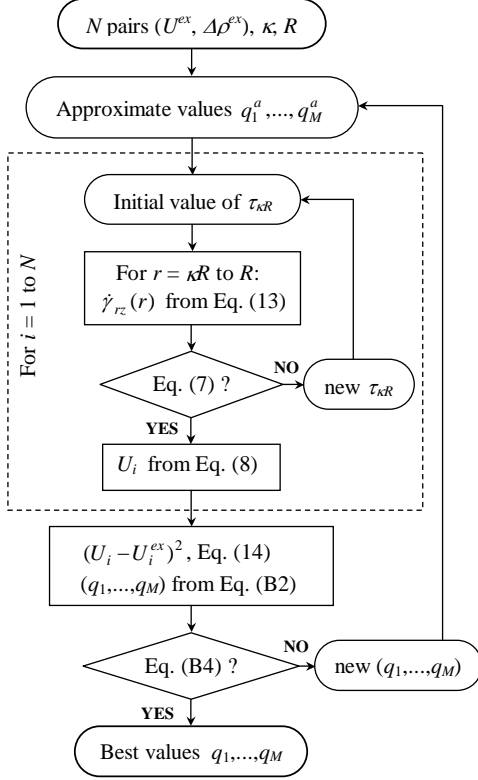
Figure 4. Flow diagram of the algorithm designed to identify the parameters of the viscosity model from experimental data of the FCV.

B. Criteria for Selecting the Apparent Viscosity Model and Initial Parameter Values

When the apparent viscosity function of a fluid is unknown, a preliminary analysis of experimental data from the FCV must be carried out in order to select the appropriate apparent viscosity model, as indicate above. In this sense, one may take advantage of the simple analytic solutions available explicitly for Newtonian fluids. Thus, for each pair $\{U^{ex}, \Delta\rho^{ex}\}$, values of both approximate viscosity function η_a and the apparent shear rate $\dot{\gamma}_a$ through the equations reported in Appendix A may be calculated. The curve $\eta_a(\dot{\gamma}_a)$ thus obtained presents a shape similar to the apparent viscosity $\eta(\dot{\gamma})$ (or true viscosity function). In this sense, it is appropriate to point out that several authors prefer to designate η_a as the apparent viscosity (a designation typically used for η) while $\dot{\gamma}_a$ has the same meaning as given in this work (see also Brunn and Vorwerk (1993) for relevant discussion concerning these functions). Then different viscosity models can be easily fitted to data $\eta_a(\dot{\gamma}_a)$, to find a set of approximate initial parameters $q_1^a,...,q_M^a$. An analysis of the fitting goodness, which is statistically measured through the determination coefficient $\hat{r}^2$, defines the suitable model for the sample considered (Berli

and Deiber, 2001). This calculation is readily performed through standard mathematical softwares.

The selection of parameter values for initialization described above is important for the iterative process used, which involves the Newton-Raphson subroutine, having into account that convergence is satisfactory as long as initial parameter values are chosen sufficiently close to the solution. In this sense, it has been shown that the approximate parameters $q_1^a,...,q_M^a$, obtained from the curve $\eta_a(\dot{\gamma}_a)$, are good choices to initialize the calculation scheme described above (Berli and Deiber, 2001; 2004). The procedure suggested here may be regarded as a form of converting the approximate model parameters into a good estimate of the true ones; i.e., one obtains $\eta(\dot{\gamma})$ from direct experimental data $\eta_a(\dot{\gamma}_a)$ through an iterative process.

C. Seudo-experimental data

Samples of synthetic data are well suited to test the procedure suggested, as the true viscosity of the fluid is known beforehand (Berli and Deiber, 2001; 2004). Thus data reported in Fig. 3 are used here to estimate the viscosity function (supposedly unknown) of the fluid. Data for a PL fluid were also obtained numerically (Function II with $q_1 = 0.2$ Pa s^n and $q_2 = 0.7$), considering a FCV with the same characteristics as those used above ($R = 0.005$ m, $\kappa = 0.25$) and $\Delta\rho$ ranging from 10 to 4000 kg/m^3. In all cases, discrete values of $U_i^{ex,f}$ vs. $\Delta\rho_i^{ex,f}$ were attained, where superscript f means error-free data here. Therefore, in order to simulate the experiments better, different levels of experimental noise δ were introduced in the velocity data by defining $U_i^{ex,\delta} = U_i^{ex,f}(1 + \delta G)$, where G is a Gaussian random number with zero mean and unit variance.
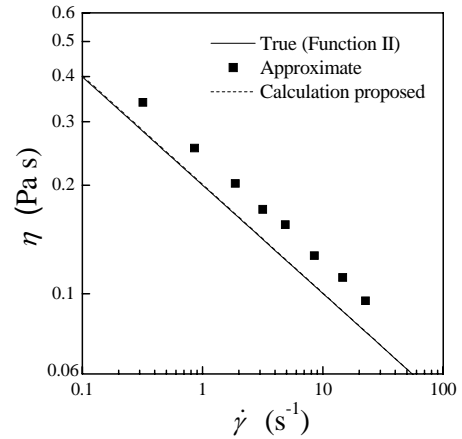

Figure 5. Apparent viscosity versus shear rate for a fluid obeying Function II, with $\delta = 0.05$. Lines represent the true and calculated viscosity functions (parameter values in Table 2). Symbols refer to the approximate values obtained by using Eqs. (A2) and (A4).

Table 2. Parameter values for different samples involving pseudo-experimental data from a FCV.

Function	Parameters	True values	$\delta = 0.01$		$\delta = 0.05$	
			Approximate	Calculated	Approximate	Calculated
II	q_1 (Pa s^n)	0.2	0.244	0.2002	0.244	0.2010
	q_2	0.7	0.699	0.7004	0.698	0.7023
	$\mathfrak{r}^2$			0.9991		0.9789
IV	q_1 (Pa s)	0.1	0.099	0.1002	0.101	0.1018
	q_2 (s)	0.05	0.032	0.0502	0.033	0.0523
	q_3	1	1.070	0.9963	1.085	0.9678
	$\mathfrak{r}^2$			0.9997		0.9925

D. Results and Discussion

The procedure described above in order to identify the parameters of the apparent viscosity models was applied to scattered data $U_i^{ex,\delta}$ vs. $\Delta\rho_i^{ex}$ of different fluids obtained as described in Section 5.3. The parameter values and the determination coefficient obtained for different levels of pseudo-experimental errors are reported in Table 2. In particular, Fig. 5 illustrates the results obtained with FCV data corresponding to a PL fluid. In this figure, the symbols represent approximate values $\eta_a(\dot{\gamma}_a)$, from which the initial parameters are estimated. Also in Fig. 5, the dashed line represents $\eta(\dot{\gamma}, q_1,..., q_M)$ with the parameter values obtained through the algorithm proposed here (Table 2), while the full line is the apparent viscosity expected. Excellent results are observed (the lines are superposed and almost indistinguishable from one another), even for the highest levels of δ (around 5%). In this sense it is also worth observing that commercial instruments provide velocity data with error levels of the order of 1 %. Fig. 5 shows that the PL model applied to sub-regions of experimental data is also comprised in our procedure, without the need of using semi-empirical correlations.

Following we consider a fluid whose apparent viscosity model involves more than two parameters; more precisely, Function IV in Table 1 is selected now. This example is used to compare our results to those obtained through the procedure currently used with FCVs (Section 2.3, Eq. (11)). For this purpose, we first obtain $D\mu/D_N$ vs. $U^{ex,\delta}/R$, from data $U^{ex,\delta}$ vs. $\Delta\rho^{ex}$, as illustrated in Fig. 6. The curve has been divided into three regions, and the flow index n associated to each region has been estimated by using Eq. (11). With these values of n, which are reported in Fig. 6, the constant K and then the effective shear rate $KU^{ex,\delta}/R$ of each region were obtained (see Section 2.3). The final viscosity curve, which consists of discrete and scattered values, is presented in Fig. 7 through symbols. This figure also includes the numerical prediction through the procedure suggested in this work (dashed line). The required parameters are reported in Table 2. It is observed that the curve of scattered data lies to the left of the true viscosity, meaning that $KU^{ex,\delta}/R$ is lower than the true shear rate $\dot{\gamma}$. This result indicates that n, obtained as an average in each region of Fig. 6, does not sense appropriately the true slope of the curve at each $\dot{\gamma}$. Thus a systematic error is introduced in the calculation of K, which is a disadvantage observed in the procedure currently used to attain the apparent viscosity with the FCV (Phan-Thien *et al.*, 1993; Zheng *et al.*, 1994). In contrast, the procedure proposed here, based on the identification of the unknown parameters, allows one to get a calculated apparent viscosity that approximates well the expected values (Fig. 7).
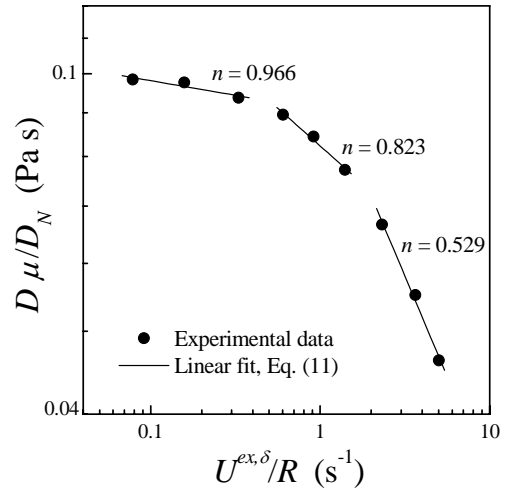

Figure 6. Apparent viscosity as a function of the ratio U/R for a fluid obeying Function IV, with $\delta = 0.01$. Symbols are the values obtained from the relative drag force. Lines represent the prediction of Eq. (11) for different intervals of U/R.
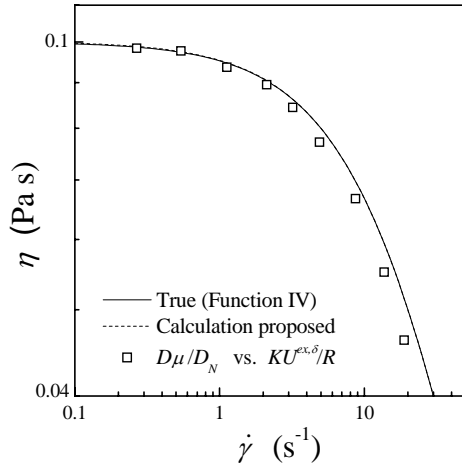
Figure 7. Apparent viscosity versus shear rate for a fluid obeying Function IV, with $\delta = 0.01$. Lines represent the true and calculated viscosity functions (parameter values in Table 2). Symbols represent the effective values obtained through the procedure involving Fig. 6 and Eq. (11) (Section 2.3).

VI. CONCLUSIONS

Although the FCV provides a simple procedure to determine the viscosity of Newtonian fluids, the calculation of the apparent viscosity $\eta(\dot{\gamma}) = \tau/\dot{\gamma}$ of non-Newtonian fluids is quite complex in this device. In fact, both τ and $\dot{\gamma}$ cannot be obtained directly from the experimental values $\{\Delta\rho, U\}$. This remarkable difference between the FCV and conventional viscometric cells motivated the search of procedures capable of solving this problem involving non-Newtonian fluids.

The present work proposes an algorithm to process data measured with the FCV for different non-Newtonian fluids. This generic procedure has been designed to perform calculations for any model of the apparent viscosity function and for any value of ratio κ. As observed in Figs. 5 and 7, the close agreement between the apparent viscosity (synthetic data) and the calculated apparent viscosity through the identification of parameters indicates the robustness of the algorithm proposed. Although apparent viscosity models were selected from Table 1 as typical examples to illustrate the study carried out here, any other model may be also used in practical situations. Indeed, the success of the procedure proposed here relies on the adequate computation of the unknown function $\dot{\gamma}(r)$ involved in the integral equation (Eq. (7)), by considering a suitable apparent viscosity model with appropriate initial parameter values.

Finally, it is worth observing that the evaluation of $\dot{\gamma}$ and then $\eta(\dot{\gamma})$ from data $\{\Delta\rho, U\}$ measured in the FCV, requires inverting an integral equation, the solution of which is not unique due to the scattering present in experimental data. In this work, instead of determin-

ing numerical values of $\eta(\dot{\gamma})$, the parameters corresponding to an apparent viscosity model (a required function to solve the FCV in the viscometric context) are identified for the fluid under study. Therefore, it is also clear that this methodology does not eliminate the difficulty associated to the existence of other possible solutions. Thus, one should not expect a unique solution but the best estimate of parameters to construct the curve $\eta(\dot{\gamma})$, from those attainable. This implies the conversion of $\eta_a(\dot{\gamma}_a)$ into $\eta(\dot{\gamma}, q_1, ..., q_M)$ through the algorithm proposed.

APPENDIX

A. Newtonian Fluids in the FCV

The use of $\tau_{rz} = \mu\dot{\gamma}_{rz}$ in the problem defined by Eqs. (7), (8) and (13) yields the following equations for the annular flow developed in the FCV (Lohrenz *et al.*, 1960; Bird *et al.*, 1977; Cristescu *et al.*, 2002),

$$u_z(r) = -U\left\{[1-(r/R)^2] + (1+\kappa^2)\ln(r/R)\right\}/\psi(\kappa), \quad (A1)$$

$$U = -\frac{\Delta\rho\, g\, (\kappa R)^2}{2\mu}\frac{\psi(\kappa)}{(1+\kappa^2)}, \quad (A2)$$

where, $\psi(\kappa) = (1-\kappa^2) + (1+\kappa^2)\ln\kappa$ is a function involving the geometric parameter κ only. Equation (A2) is important in practice to determine the viscosity μ from experimental data U versus $\Delta\rho$ in the characterization of Newtonian fluids.

From the above equations, the rheometric shear stress and shear rate for a Newtonian fluid at $r = \kappa R$ (surface of the falling cylinder) are readily derived, i.e.,

$$\tau_{\kappa R} = -\frac{\Delta\rho\, g\kappa R}{2}\left(\frac{1-\kappa^2}{1+\kappa^2}\right), \quad (A3)$$

$$\dot{\gamma}_{\kappa R} = \frac{U}{\kappa R}\frac{(1-\kappa^2)}{\psi(\kappa)}. \quad (A4)$$

Also for Newtonian fluids, the drag force $D = \Delta\rho g(\kappa R)^2 \pi L$ (Phan-Thien *et al.*, 1993; Zheng *et al.*, 1994) can be written in terms of μ and U as,

$$D_N = -2\pi L\mu U(1+\kappa^2)/\psi(\kappa). \quad (A5)$$

B. Subroutine to Identify the Viscosity Model Parameters in the FCV

In order to identify the set of M parameters that makes the sum S (Eq. (14)) as small as possible, the following functions must be minimized simultaneously,

$$F_j = \frac{dS}{dp_j} = \sum_{i=1}^{N}\frac{2}{U_i^{ex}}\left(\frac{U_i - U_i^{ex}}{U_i^{ex}}\right)\frac{dU_i}{dp_j}, \quad (B1)$$

where $j = 1$ to M. By defining $\mathbf{F} = [F_1, ..., F_M]^T$ and $\mathbf{q} = [q_1, ..., q_M]^T$, the problem to be solved is expressed, $\mathbf{F}(\mathbf{q}) = 0$. The best estimate of $\mathbf{q}$ is obtained with the Newton-Raphson subroutine for systems of non-linear algebraic equations (Carnahan *et al.*, 1969). This method involves an iterative process in which $\mathbf{q}$ is modified through the following recurrence law,

$$q^{(l+1)} = q^{(l)} - F'(q^{(l)})^{-1} \cdot F(q^{(l)}), \qquad (B2)$$

starting from an initial vector $q^{(0)}$, here included as the vector of approximate values $q^{(a)}$. In Eq. (B2), $F' = dF/dq$ is a symmetrical matrix of dimensions $M \times M$ that is inverted through the Gaussian elimination subroutine (Carnahan *et al.*, 1969). The components of this matrix are given by,

$$F'_{jk} = \sum_{i=1}^{N} \frac{2}{U_i^{ex}} \left[\frac{1}{U_i^{ex}} \frac{dU_i}{dq_k} \frac{dU_i}{dq_j} + \left(\frac{U_i - U_i^{ex}}{U_i^{ex}} \right) \frac{d^2 U_i}{dq_k dq_j} \right],$$

$$(B3)$$

where $k = 1$ to M. The iterative process ends when,

$$\left| (q^{(l+1)} - q^{(l)})/q^{(l)} \right| \leq \xi, \qquad (B4)$$

with a value of ξ sufficiently small ($\sim 10^{-3}$), as shown in the diagram of Fig. 4.

The derivatives dU_i/dq_j and $d^2U_i/(dq_k dq_j)$ in Eqs. (B1) and (B3) are obtained numerically through the finite differences method. Backward differences Δq are used to make these calculations, for instance, $dU_i/dq_1 = [U_i(q_1+\Delta q_1, q_2,..., q_M) - U_i(q_1, q_2,..., q_M)]/\Delta q_1$. This implies that M^2+M different values of U_i must be calculated for each $\Delta \rho_i^{ex}$ data. That is, $U_i(q_1, q_2,..., q_M)$, $U_i(q_1+\Delta q_1, q_2,..., q_M)$, ... $U_i(q_1, q_2,..., q_M +\Delta q_M)$.

REFERENCES

Ashare, E., Bird, R.B. and Lescarboura, J.A. "Falling cylinder viscometer for non-Newtonian fluids." *AIChE J.,* **11**, 910 (1965).

Berli, C.L.A. and Deiber, J.A. "A procedure to determine the viscosity function from experimental data of capillary flow." *Rheol. Acta,* **40**, 272 (2001).

Berli, C.L.A. and Deiber, J.A. "Theoretical analysis of the gravity-driven capillary viscometer." *Rev. Sci. Instrum.,* **75**, 976 (2004).

Bird, R.B., Armstrog, R. and Hassager, O. *Dynamics of Polymeric Liquids*, Vol. 1, J. Wiley & Sons., New York (1977)

Brunn, P.O. and Vorwerk, J. "Determination of the steady-state shear viscosity from measurements of the apparent viscosity for some common types of viscometers." *Rheol. Acta.,* **32**, 380 (1993).

Carnahan, B., Laither, H. and Wilkies, J. *Applied Numerical Methods*, Wiley, New York (1969).

Chan, R.K.Y. and Jackson, D.A. "An automated falling-cylinder high pressure laser-Doppler viscometer." *J. Phys. E: Sci. Instum.,* **18**, 510 (1985).

Chen, M.C.S. and Swift, G.W. "Analysis of entrance and exit effects in a falling cylinder viscometer." *AIChE J.,* **18**, 146 (1972).

Cho, K., Cho, Y.I. and Park, N.A. "Hydrodynamics of a vertically falling thin cylinder in non-Newtonian fluids." *J. Non-Newtonian Fluid Mech.,* **45**, 105 (1992).

Cristescu, N.D., Conrad, B.P. and Tran-Son-Tay, R. "A closed form solution for falling cylinder viscometers." *Int. J. Eng. Sci.,* **40**, 605 (2002).

Cross, M.M. "Rheology of non-Newtonian fluids: a new flow equation for pseudoplastic systems." *J. Colloid Sci.,* **20**, 417 (1965).

Davis, A.M.J. and Brenner, H. "The falling-needle viscometer." *Phys. Fluids.,* **13**, 3086 (2001).

Eichstadt, F.J. and Swift, G.W. "Theoretical analysis of the falling cylinder viscometer for power law and Bingham plastic fluids." *AIChE J.,* **12**, 1179 (1966).

Friedrich, C., Honerkamp, J. and Weese, J. "New ill-posed problems in rheology." *Rheol. Acta.,* **35**, 186 (1996).

Ilic, V. and Phan-Thien, N. "Viscosity of concentrated suspensions of spheres." *Rheol. Acta.,* **33**, 283 (1994).

Lohrenz, J., Swift, G.W. and Kurata, F. "An experimentally verified theoretical study of the falling cylinder viscometer." *AIChE J.,* **6**, 547 (1960).

Macosko, W.K. *Rheology: principles, measurements and applications*, VCH Publisher Inc., New York (1994).

Park, N.A. and Irvine Jr., J.F. "Measurements of rheological fluid properties with the falling needle viscometer." *Rev. Sci. Instrum.,* **59**, 2051 (1988).

Park, N.A. and Irvine Jr., J.F. "Falling cylinder viscometer end correction factor." *Rev. Sci. Instrum.,* **66**, 3982 (1995).

Phan-Thien, N., Jin, H. and Zheng, R. "On the flow past a needle in a cylindrical tube." *J. Non-Newtonian Fluid Mech.,* **47**, 137 (1993).

Sha, Z.S. "The improvement on the falling needle viscometer." *Rev. Sci. Instrum.,* **68**, 1809 (1997).

Tanner, R.I. *Engineering Rheology*, Oxford University Press, Oxford (1985).

Walters, K. *Rheometry*, J. Wiley & Sons, New York (1975).

Wehbeh, E.G., Ui, T.J. and Hussey, R.G. "End effects for the falling cylinder viscometer." *Phys. Fluids A.,* **5**, 25 (1993).

Zheng, R., Phan-Thien, N. and Tanner, R.I. "The flow past a sphere in a cylindrical tube: effects of inertia, shear thinning and elasticity." *Rheol. Acta,* **30**, 499 (1991).

Zheng, R., Phan-Thien, N. and Ilic, V. "Falling needle rheometry for general viscoelastic fluids." *J. Fluids Eng.,* **116**, 619 (1994).